Available online at www.sciencedirect.com
SCIENCE DIRECT
Developmental Biology 294 (2006) 352–365
DEVELOPMENTAL BIOLOGY
www.elsevier.com/locate/ydbio

C. elegans Kallmann syndrome protein KAL-1 interacts with syndecan and glypican to regulate neuronal cell migrations

Martin L. Hudson [a], Tarja Kinnunen [b], Hediye Nese Cinar [a], Andrew D. Chisholm [a,*]

[a] *Department of Molecular, Cell, and Developmental Biology, Sinsheimer Laboratories, University of California, Santa Cruz, CA 95064, USA*
[b] *School of Biological Sciences, University of Liverpool, Bioscience Building, Crown Street, Liverpool L69 7ZB, UK*

Received for publication 20 December 2005; revised 17 February 2006; accepted 21 February 2006
Available online 3 May 2006

Abstract

The anosmin-1 protein family regulates cell migration, axon guidance, and branching, by mechanisms that are not well understood. We show that the *C. elegans* anosmin-1 ortholog KAL-1 promotes migrations of ventral neuroblasts prior to epidermal enclosure. KAL-1 does not modulate FGF signaling in neuroblast migration and acts in parallel to other neuroblast migration pathways. Defects in heparan sulfate (HS) synthesis or in specific HS modifications disrupt neuroblast migrations and affect the KAL-1 pathway. KAL-1 binds the cell surface HS proteoglycans syndecan/SDN-1 and glypican/GPN-1. This interaction is mediated via HS side chains and requires specific HS modifications. SDN-1 and GPN-1 are expressed in ventral neuroblasts and have redundant roles in KAL-1-dependent neuroblast migrations. Our findings suggest that KAL-1 interacts with multiple HSPGs to promote cell migration.

Keywords: Morphogenesis; Ephrin; Syndecan; Glypican; Kallmann syndrome; Anosmin; Heparan sulfate proteoglycan

Introduction

Anosmins are a family of conserved secreted proteins that regulate cell migration and axon branching. Anosmin was first identified as being defective in human Kallmann syndrome (KS), a genetic disease combining anosmia and hypogonadism. The gonadal defects in KS patients result from lack of pituitary gonadotrophic hormones (hypogonadotrophic hypogonadism) (Gonzalez-Martinez et al., 2004a; MacColl et al., 2002; Rugarli, 1999). During development, olfactory sensory neurons extend axons in the lateral olfactory tract (LOT) towards the rostral telencephalon and then, after a delay, defasciculate and send collateral branches into the developing olfactory bulb (OB) (Key and St John, 2002). In KS patients, the final phase of branching into the OB is thought to be defective (Schwanzel-Fukuda et al., 1989).

Kallmann syndrome is genetically heterogeneous, with X-linked recessive, autosomal dominant, and autosomal recessive forms known. Recessive X-linked KS is caused by mutations in the *KAL1* gene (Franco et al., 1991; Hardelin et al., 1992, 1993; Legouis et al., 1991), which encodes a secreted protein, anosmin-1. Anosmin-1 defines a conserved family of proteins that contain a whey acidic protein-like motif (the WAP domain) found in serine protease inhibitors, and four fibronectin type III (FNIII) repeats. Anosmin-1 is secreted by neurons of the OB and localizes to the extracellular matrix of the OB (Hardelin et al., 1999), suggesting it acts as a short-range signal for LOT axons that induces their branching as they pause at the surface of the telencephalon. In explant assays, anosmin-1 stimulates branching of both LOT and OB neurons (Soussi-Yanicostas et al., 2002).

How does anosmin-1 affect axon outgrowth, branching, and cell migration? Several lines of evidence suggest that anosmin-1 function may involve heparan sulfate proteoglycans (HSPGs). Anosmin-1 binding to membrane fractions of neurons can be competed with heparin, and anosmin-1 binds heparan sulfate (HS) with nanomolar affinity (Hu et al., 2004; Soussi-Yanicostas et al., 1996, 1998). However, specific HSPGs involved in anosmin-1 functions have not yet been identified. Furthermore, it has not yet been resolved whether HSPGs are the cellular receptors for anosmin-1, whether they mediate an

* Corresponding author.
E-mail address: chisholm@biology.ucsc.edu (A.D. Chisholm).

0012-1606/$ - see front matter © 2006 Elsevier Inc. All rights reserved.
doi:10.1016/j.ydbio.2006.02.036

interaction of anosmin-1 with another signaling receptor, or whether HSPGs solely act to localize or anchor anosmin-1.

The genetic basis of autosomal dominant KS has recently been traced to *FGFR1*, encoding a fibroblast growth factor receptor (Dode et al., 2003). The involvement of FGFR1 and anosmin-1 in the same syndrome suggests that anosmin-1 might affect FGFR signaling (Dode and Hardelin, 2004). Anosmin-1 can stimulate FGFR1 signaling in human neuroblasts (Gonzalez-Martinez et al., 2004b). Tissue-specific deletion of *Fgfr1* in the telencephalon causes defects in OB morphogenesis (Hebert et al., 2003), reminiscent of KS. However, unlike KS, olfactory axons enter the OB in the mouse *Fgfr1* mutants, suggesting that the mechanisms of autosomal dominant and X-linked recessive KS may differ.

Invertebrate anosmin-1 orthologs have been found in *C. elegans* (Rugarli et al., 2002) and in *Drosophila* (Andrenacci et al., 2004). The *C. elegans* gene *kal-1* has been shown to affect epidermal morphogenesis, development of male tail sensilla, and axon branching (Rugarli et al., 2002). Overexpression of KAL-1 in certain neurons causes enhanced branching (Bulow et al., 2002). A genetic screen for suppressors of KAL-1-induced branching recovered mutations in genes required for secondary modifications of HS: *hst-6,* encoding the *C. elegans* HS-6-O-sulfotransferase, and *hse-5*, which encodes HS glucuronyl C-5 epimerase (Bulow et al., 2002). Loss of function of these enzymes prevents KAL-1-induced branching, suggesting that HSPGs are essential for KAL-1 action.

The embryonic defects of *kal-1* mutants resemble those of ephrin signaling mutants, which affect epidermal morphogenesis by regulating development of the substrate neuroblasts. To decipher the relationship of KAL-1 and ephrin signaling, we have examined the role of *kal-1* in embryonic morphogenesis. We find that *kal-1* mutants display delayed migration of the ventral neuroblasts (VNBs) that generate the substrate for epidermal epiboly. Our analysis suggests KAL-1 does not modulate Eph or FGF signaling. We show that specific HS modifications play distinct roles in VNB migration, acting in a KAL-1-dependent process. By biochemical and genetic assays, we show that KAL-1 interacts with the HSPGs syndecan and glypican in embryonic neuroblast migrations.

Materials and methods

Genetics and phenotypic quantitation

The wild-type strain used is Bristol N2 (Brenner, 1974). All strains were maintained at 20°C on NGM agar under standard conditions. The following previously described mutations were used: LG I: *kal-1(gb503)*, *mab-20(ev574)*; LG II: *vab-1(e2027)*, *ptp-3(mu256)*; LG III: *hse-5(tm472)*; LG IV: *efn-1(e96)*; LG X: *sdn-1(ok449)* (Minniti et al., 2004), *sdn-1(zh20)* (Rhiner et al., 2005), *hst-2(ok595), hst-6(ok273), sax-3(ky123), egl-15(n1456)* and *lin-15(n765ts)*. Double and triple mutants were constructed using standard genetic methods. Deletion alleles were genotyped by three primer multiplex PCR (with one primer located in the deletion) to identify mutant and wild type alleles in a single reaction. Primer sequences are available on request.

The following transgenes were used: *otIs33*[P*kal-1*-GFP], *otIs81*[P*unc119*-KAL-1], *otEx1254[egl-15(5B)+ceh-22*::*GFP]* (Bulow et al., 2004), *oxIs12*.

In addition to *gb503*, a second *kal-1* allele, *ok1056,* was isolated by the *C. elegans* Gene Knockout Consortium. We determined the breakpoints of *kal-1 (ok1056)* and found it to be a 1033 bp deletion with a 33 bp insertion, with genomic breakpoints 5′ AGTTTTCGATGATTTTGCGG/ATGAGAATT-TGGCGCCAGGA 3′. *ok1056* deletes most of exon 5, affecting the second and third FNIII repeats.

Quantitation of lethal and morphological phenotypes was performed as described (George et al., 1998). All analyses of penetrance are based on counts of multiple (3–6) complete broods from animals raised at 20°C from outcrossed strains; $n > 500$ animals for each genotype. Timelapse analysis of embryogenesis was performed as described (Chin-Sang et al., 2002) at 20°C; $n = 10$–30 per genotype for all quantitative analysis of embryogenesis. *kal-1(gb503)* was previously reported to cause ~26% embryonic lethality in a *him-8(e1489)* background, compared with 13% embryonic lethality for *him-8(e1489)* alone. After outcrossing we found that neither *gb503* or *ok1056* caused significant embryonic lethality (Table 1).

Characterization of C. elegans glypican GPN-1

The *C. elegans* gene F59D12.4 encodes a member of the glypican family. We confirmed the *gpn-1* gene structure by sequencing the cDNA yk747a2. The predicted GPN-1 protein is 543 amino acid residues, with a molecular weight of 58.5 kDa after removal of signal sequences for secretion and GPI anchorage. GPN-1-specific bands in SDS-PAGE gels are smaller (30–35 kDa, Fig. 3C). HSPGs are known to run anomalously in SDS-PAGE; additionally, glypicans are often processed by proprotein convertases (De Cat et al., 2003), and GPN-1 contains several potential cleavage sites.

Three alleles of *gpn-1* have been isolated by reverse genetics. *ok377*, generated by the Gene Knockout Consortium, is a 1195-bp deletion of part of exon 3. *tm595* (S. Mitani) deletes part of exon 2 and all of exon 3, and *tm588* deletes exon 4. All three mutations cause no overt defects in epidermal morphogenesis apart from variation in embryo size (not shown). To assay complementation of the *gpn-1(ok377)* phenotype we rescued the synthetic lethality of *efn-4 ok377* double mutants. We generated transgenic arrays by

Table 1
kal-1 synergizes with null mutations in components of known VNB migration pathways

Genotype	Embryonic lethality (%) ±SEM	Larval lethality (%) ±SEM	Adult Vab morphology (%) ±SEM
Wild type	0.1 ± 0.1	0.1 ± 0.1	0.1 ± 0.2
kal-1(gb503)	0.6 ± 0.6	0.2 ± 0.2	5.6 ± 0.7
vab-1(e2027)	44.4 ± 2.8	22.8 ± 3.2	31.0 ± 3.0
kal-1 vab-1	54.6 ± 2.5*	32.6 ± 1.8*	12.4 ± 1.4
efn-1(e96)	22.4 ± 2.9	14.1 ± 1.9	50.3 ± 1.3
kal-1 efn-1	27.7 ± 7.7	37.2 ± 1.8***	29.3 ± 2.9
efn-4(bx80)	11.5 ± 1.1	9.0 ± 1.8	31.2 ± 1.7
kal-1 efn-4	35.3 ± 4.2***	24.1 ± 2.5***	26.2 ± 1.4
mab-20(ev574)	19.8 ± 2.1	32.7 ± 1.3	27.7 ± 1.2
kal-1 mab-20	27.0 ± 0.2**	29.5 ± 2.9	34.7 ± 1.3***
ptp-3(mu256)	5.5 ± 1.4	1.1 ± 0.5	4.5 ± 0.4
kal-1 ptp-3	8.7 ± 0.8	4.4 ± 1.2**	11.4 ± 1.4***
sax-3(ky123)	46.4 ± 4.3	31.8 ± 2.4	16.1 ± 2.4
kal-1 sax-3	57.9 ± 3.9 ns	37.0 ± 2.8 ns	4.3 ± 1.3

The penetrance of at least one morphogenetic phenotype (embryonic lethality, larval lethality or aberrant epidermal morphology in adults) was enhanced in a *kal-1(gb503)* background relative to the single mutant alone. The enhancement of total (embryonic plus larval) lethality in *sax-3 kal-1* is highly significant relative to *sax-3* alone, although the individual measures are not significantly different. In some double mutant combinations (e.g., *kal-1 vab-1, kal-1 sax-3*) the fraction of animals with adult Vab phenotypes is lower than the control because an increased fraction of the population died earlier in development. All mutations used are null, by genetic or molecular criteria (see Materials and methods). Genotypes were compared by Student's *t* test; *$P < 0.05$, **$P < 0.01$, ***$P < 0.005$; all comparisons are between the matched *kal-1(+)* and *kal-1(−)* strains.

injection of the *gpn-1* cosmid C03H12 (1 ng/μl), *sur-5*: :GFP marker (10 ng/μl), and pBluescript (20 ng/μl) into *efn-4(bx80); gpn-1(ok377)* double mutants. Multiple lines were generated, and scored for rescue of embryonic lethality: *efn-4(bx80); gpn-1(ok377); juEx955* strains displayed 7.2 ± 1.9% embryonic lethality compared with 26.4 ± 5.3% for *efn-4(bx80); gpn-1(ok377)*. These data establish that the enhancement of *efn-4* embryonic lethality results from the *ok377* mutation.

Analysis of HSPG expression

The functional SDN-1: :GFP reporter (*jtEx36*) consists of full length SDN-1 tagged at the C-terminus with GFP. Arrays containing SDN-1: :GFP rescue *sdn-1(ok449)* phenotypes and will be described in detail elsewhere (T.K., in preparation). To generate glypican reporters, 4.3 kb of the *gpn-1* promoter region was amplified and cloned into the pCR8/GW/TOPO entry vector (Invitrogen). The insert was recombined into the pCZGY32 destination vector (a gift from G. Gallegos) which contains Venus YFP open reading frame and the *unc-54* 3′untranslated region, to yield plasmid pCZGY50. Transgenic arrays were generated by co-injecting pCZGY50 at 10 ng/μl, and the *lin-15(+)* plasmid pJM23 (Huang et al., 1994) (50 ng/μl) into *lin-15(n765ts)* mutants. Two independent lines were isolated (*juEx900* and *juEx901*) which showed similar expression patterns. To make GPN-1: :GFP we used a modular Gateway based destination vector (pCZGY20) containing the KAL-1 N-terminal signal sequence (residues 1–15) followed by Venus YFP (Nagai et al., 2002). A multiple cloning site allows insertion of promoters and the Gateway recombination sites allow insertion of ORFs for secreted proteins. We amplified the GPN-1 ORF and cloned it into pCR8/GW/TOPO. The GPN-1 ORF was then recombined into a version of pCZGY20 containing the *gpn-1* promoter to create pCZGY41, which was injected at 1 ng/μl with P*ttx-3*-RFP (Altun-Gultekin et al., 2001) to create the array *juEx1108*. Rescue of the *gpn-1(ok377)* phenotype was confirmed in the *efn-4(bx80)* background as above. For immunostaining of GFP transgenic animals, we used standard procedures (Finney and Ruvkun, 1990); rabbit anti-GFP (Molecular Probes, A11122) was used at 1:1000 dilution and MH27 supernatant at 1:100. Staining was visualized with appropriately conjugated 2° antisera on a Zeiss Axioplan 2 or a Zeiss Pascal confocal microscope.

HSPG biochemistry

Recombinant KAL-1: :Fc was prepared by transient transfection of 293T cells with the pCXFc-KAL plasmid (Bulow et al., 2002). Protein was harvested 48 h post-transfection, centrifuged to remove cellular debris and 0.5 volumes of 3× binding buffer added (final concentrations: 50 mM HEPES pH 7.4, 500 mM NaCl, 0.1% Tween-20, 1 mM PMSF, 1× Complete EDTA-free protease inhibitor cocktail, Roche Diagnostics). KAL-1: :Fc was bound to protein-A agarose (Roche Diagnostics) overnight at 4°C, washed once with 1× binding buffer and once with high salt binding buffer (composition as above but with 1 M NaCl). To minimize proteolysis, the affinity matrix was freshly prepared for each experiment.

Embryos were isolated by alkaline lysis from gravid adults grown in 50 ml liquid culture in 25 × 25 cm trays. Embryonic tissue was prepared by sonication in 50 mM Tris–HCl, pH 7.5, 150 mM NaCl, 1% Nonidet P-40, 1 mM EDTA, 1 mM PMSF, 1× Complete EDTA-free protease inhibitor cocktail, Roche Diagnostics and allowed to solubilize for 5 h at 4°C. Samples were centrifuged at 10 000×*g* for 20 min and the supernatants bound to protein-A agarose-KAL-1: :Fc affinity matrix overnight at 4°C. Samples were washed with lysis buffer containing 0.25 M NaCl and eluted using 1.5 M NaCl in lysis buffer, and the eluate desalted in water on a NAP-5 sephadex column (Amersham). Samples were concentrated using a SpeedVac, resuspended in 1× heparitinase buffer (100 mM sodium acetate pH 7.0, 0.1 mM calcium acetate) and digested overnight at 37°C with 2.5 mU heparitinase I (Seikagaku, Tokyo, Japan). Samples were separated on 12% SDS-PAGE gels, blotted to PVDF membrane and allowed to dry overnight at room temperature. After blocking in 2% non-fat milk in TBSTw, samples were probed with 1:1000 3G10 (mouse anti-HS-stub antibody, Seikagaku) for 2 h followed by 1:2500 HRP conjugated sheep anti-mouse (Amersham) for 30 min. Western blots were visualized using the ECL system (Amersham).

Results

KAL-1 is required for normal migrations of ventral neuroblasts independent of FGF signaling

Loss of function in the *C. elegans* anosmin-1 ortholog *kal-1* has been previously reported to result in low penetrance defects in embryonic epidermal morphogenesis that resemble those of Eph signaling mutants (Rugarli et al., 2002). The primary developmental defects in Eph signaling mutants are in migrations of ventral neuroblasts (VNBs) following gastrulation and prior to epidermal enclosure (Chin-Sang et al., 1999; George et al., 1998). During gastrulation, endodermal and mesodermal cells migrate to the center of the developing embryo, leaving a cleft on the ventral surface flanked by VNBs (Fig. 1) (Nance and Priess, 2004). This gastrulation cleft is closed by short-range migrations of VNBs (Chisholm and Hardin, 2005) that require several partly redundant cell signaling pathways (Chin-Sang et al., 1999, 2002; George et al., 1998; Harrington et al., 2002), as well as pathways related to actin remodeling (Withee et al., 2004). If VNBs are mispositioned at the end of enclosure, as in the above mutants, epidermal cells fail to make correct contacts with their contralateral partners, leaving a hole in the ventral surface of the epidermis and leakage of internal cells. However, short delays in VNB migrations are often compatible with epidermal enclosure.

We examined embryos mutant for the putative genetic null mutation *kal-1(gb503)* using 4D time-lapse microscopy and found that although early gastrulation movements and the onset of VNB migrations were normal, closure of the gastrulation cleft was delayed compared to wild type (Figs. 1A, C, D). Despite this delay, the gastrulation cleft closed before epidermal enclosure in *kal-1* mutants and all animals underwent epidermal enclosure and elongation. A second deletion allele, *kal-1 (ok1056)* causes VNB migration defects indistinguishable from those of *kal-1(gb503)* (Fig. 1D); all analyses below use *kal-1 (gb503)*. The similarity of phenotype of two independent deletion alleles suggests that these phenotypes are caused by elimination of KAL-1 function and that KAL-1 promotes VNB cell migrations.

The *kal-1* promoter is active in many cells in the embryo (Bulow et al., 2002; Rugarli et al., 2002); using timelapse analysis, we found that *kal-1* is expressed in most VNBs from mid gastrulation stages onwards (Fig. 1B). KAL-1 is predicted to be GPI-anchored to the cell membrane and is restricted to the surfaces of cells that express it (Bulow et al., 2002). Thus, KAL-1 likely acts locally on the surfaces of VNBs to promote their migrations. Overexpression of KAL-1 from a pan-neural promoter causes epidermal morphogenetic defects (Bulow et al., 2002). We found that these likely result from VNB migration defects (Fig. 1D). The defects caused by pan-neural KAL-1 were further enhanced in a *kal-1(gb503)* background (not shown), indicating that overexpression or misexpression of KAL-1 interferes both with normal KAL-1 signaling and additional pathways involved in VNB migration. These results are consistent with KAL-1 functioning cell

autonomously or locally among VNBs to regulate their movements.

As anosmin-1 has been linked to FGF signaling in humans, we tested whether loss of FGF signaling affects VNB migrations. In *C. elegans*, a single locus, *egl-15,* encodes two FGF receptor isoforms, EGL-15A and EGL-15B (Goodman et al., 2003). Null mutations in *egl-15* confer early larval lethality reflecting the essential function of LET-756/EGL-15B signaling (Huang and Stern, 2004). VNB migrations in *egl-15* null mutant embryos derived from heterozygous mothers were normal (Fig. 1D). To address the possibility of maternal rescue of *egl-15* function, we also analyzed VNB migrations in *egl-15* mutant embryos derived from mothers that had lost *egl-15* function in the germline, and observed normal VNB migrations. We conclude that FGF signaling does not influence VNB migration, and therefore that KAL-1 is unlikely to act through FGFR in this context.

We then tested whether *kal-1* interacted with four pathways known to function in both embryonic VNB migrations and in axon guidance: the VAB-1/Eph receptor-EFN-1/ephrin pathway (Chin-Sang et al., 1999; George et al., 1998), the PTP-3 (LAR-like RPTP) pathway (Harrington et al., 2002), the ephrin EFN-4, which may act in MAB-20/Semaphorin 2A signaling (Chin-Sang et al., 2002; Ikegami et al., 2004), and SAX-3/Robo signaling (Ghenea et al., 2005). In all double mutants tested, *kal-1(gb503)* significantly enhanced VNB migration defects, epidermal enclosure defects, and embryonic lethality relative to the single mutants (Fig. 1E; Supplemental Fig. 1; Table 1). As *kal-1* enhances null mutations in these genes, KAL-1 is unlikely to act solely as a component of the Eph, LAR, EFN-4/semaphorin 2A, or Robo pathways. KAL-1 instead acts in parallel to promote a common process in VNB migration.

Heparan sulfate synthesis and specific HS modifications are important for neuroblast migrations

Both mammalian anosmin-1 and *C. elegans* KAL-1 have been linked to heparan sulfate proteoglycans (HSPGs) (Bulow et al., 2002; Soussi-Yanicostas et al., 1996, 1998). To test if HSPGs were required for embryonic VNB migrations we first examined mutants defective in HS synthesis or modification. *C. elegans* enzymes catalyzing all known steps in HS synthesis and modification have been identified (Bulow and Hobert, 2004), and deletion alleles of the genes are available (Fig. 2A). Promoters for *hst-2, hse-5*, and *hst-6* are active in multiple tissues during embryogenesis (Bulow and Hobert, 2004).

Embryos lacking the enzymes required for HS polymerization (RIB-1, RIB-2) (Morio et al., 2003) or for deacetylation and N-sulfation of glucosamine (HST-1) display defects in VNB movements much more severe than those of *kal-1* mutants (M.L.H. and A.D.C., unpublished results), showing that HSPGs are essential for VNB migrations. In contrast, mutants lacking the glucuronic acid C5 epimerase HSE-5 or the sulfotransferases HST-2 and HST-6 are mostly viable and display low-penetrance defects in epidermal morphogenesis (Table 2); we refer to this group of genes as HS modification genes. In timelapse analysis of VNB migrations, lack of HSE-5 C5 epimerase caused the most dramatic defects within this group, with a mean gastrulation cleft duration of 96 ± 7 min (Figs. 2C, D) and 6 ± 2% embryonic lethality (Table 2). *kal-1 hse-5* double mutants were not significantly different from *hse-5* single mutants either in overall lethality or in VNB migration, suggesting that KAL-1 function in morphogenesis involves C5-epimerized HSPGs. *hst-6* mutants displayed milder VNB migration defects (mean cleft duration 86 ± 7 min). *hst-6 kal-1* double mutants resemble *hst-6* single mutants, implying that the HSPGs involved in KAL-1 function are also 6-O-sulfated. In these mutants, onset of cleft opening was normal relative to E daughter ingression, but closure was delayed (Fig. 2B). A mutation in *hst-2* did not significantly affect VNB migrations, yet *hst-2 kal-1* double mutants were enhanced relative to *kal-1*, suggesting 2-O-sulfated HSPGs have cryptic roles in VNB migration.

Because *kal-1* and HS modification mutations confer relatively mild effects as single mutants, lack of enhancement in a double mutant might reflect additivity, and thus does not necessarily imply a common pathway. As a more sensitive test of whether *kal-1* and HS modification mutations affect a common pathway, we constructed triple mutants of genotype *efn-4 kal-1 mut*. Because *kal-1* strongly enhances *efn-4* phenotypes, mutations affecting the *kal-1* pathway should also enhance *efn-4* but should not further enhance an *efn-4 kal-1* double mutant. We found that HS modification mutations dramatically enhanced *efn-4* phenotypes (Table 1). *hst-6* enhanced *efn-4* embryonic phenotypes to the same extent as *kal-1*, and a *kal-1 efn-4 hst-6* triple mutant resembled *kal-1 efn-4* in overall lethality (Table 2) and VNB migration, consistent with 6-O-sulfated HSPGs acting in a KAL-1 pathway to promote VNB migration. *hse-5 efn-4* double mutants displayed enhanced morphogenetic phenotypes relative to *kal-1 efn-4* and were indistinguishable from *kal-1 hse-5 efn-4* triple mutants (Table 2). These data are consistent with KAL-1 functioning via C5-epimerized HSPGs, and also suggest that HSE-5 has other HSPG targets in addition to those involved in KAL-1 signaling. Finally, *hst-2 efn-4* double mutants show significantly higher embryonic lethality relative to *efn-4* alone, and a *kal-1 efn-4 hst-2* triple mutant is further enhanced, consistent with KAL-1 and 2-O-sulfated HSPGs acting in parallel pathways (Table 2).

In summary, the different HS modifications have different roles in VNB migration and in the KAL-1 pathway. HSPGs modified by either HSE-5 and/or HST-6 promote VNB migrations; loss of HSE-5 function has the strongest effects, paralleling its requirement in axon guidance (Bulow and Hobert, 2004). Our double mutant analysis argues that KAL-1 interacts with 6-O-sulfated HSPGs; HSPGs modified by C-5-epimerase likely have additional roles. Lack of HST-2 has no obvious effect, but synergizes with *kal-1* mutations and with *efn-4* mutations, suggesting a cryptic role for 2-O-sulfated HSPGs.

KAL-1 binds HSPGs syndecan/SDN-1 and glypican/GPN-1 via an HS dependent interaction

Our studies suggested that KAL-1 acts with one or more HSPGs in VNB migration. *C. elegans* encodes at least four potential HSPG core proteins: the cell surface HSPGs syndecan/SDN-1 (Minniti et al., 2004; Rhiner et al., 2005) and glypican/GPN-1 (Fig. 3A; Materials and methods), and the basement membrane HSPGs perlecan (Rogalski et al., 1993) and collagen XVIII/CLE-1 (Ackley et al., 2001). Of these only SDN-1 has been shown to be decorated by heparan sulfate chains (Minniti et al., 2004). To determine which HSPGs interacted with KAL-1

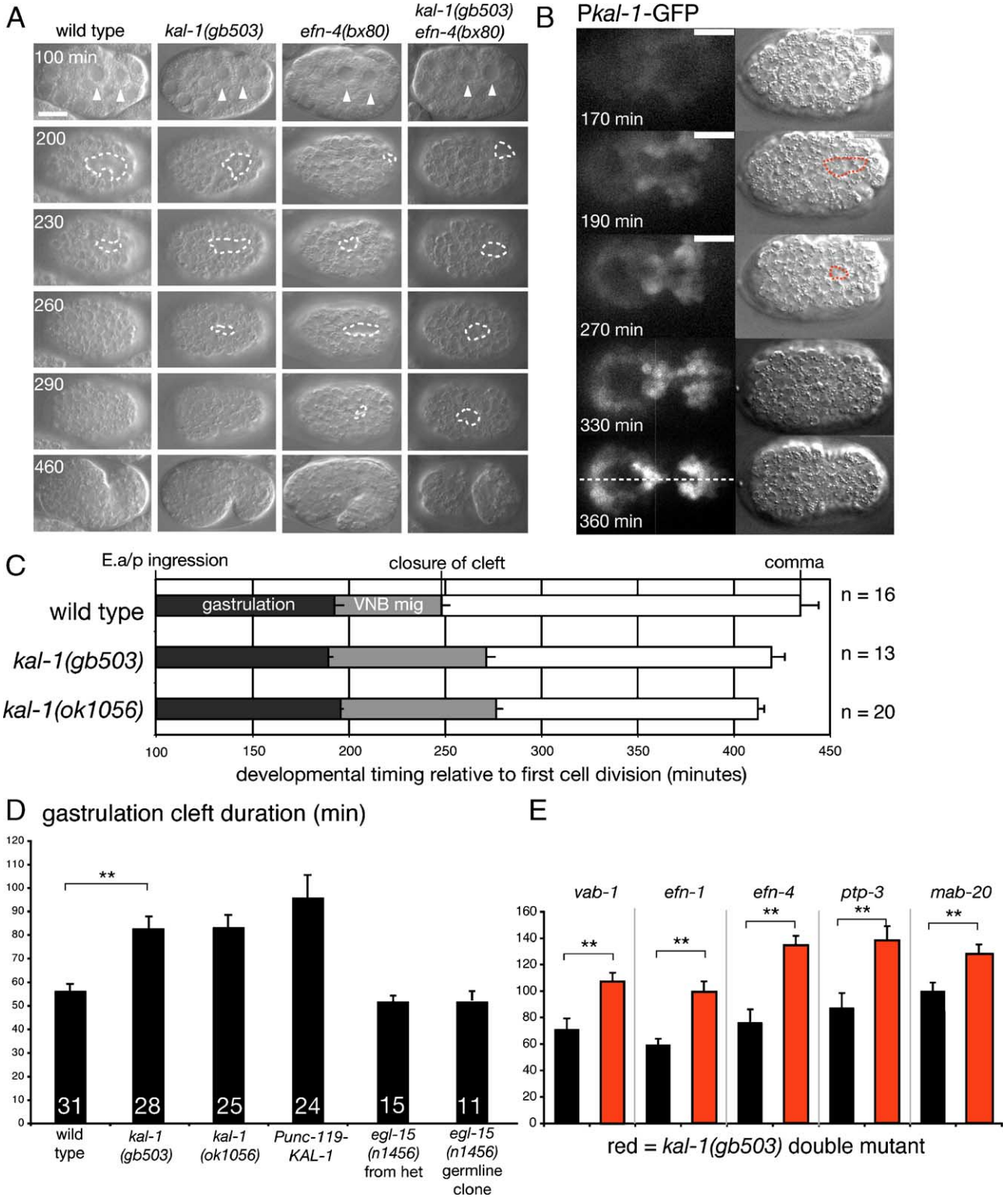

we first used affinity chromatography. We expressed KAL-1∷Fc in HEK293 cells and showed that it is N-glycosylated and binds heparin in vitro (Fig. 3B). We coupled KAL-1∷Fc to a solid matrix and passed extracts of *C. elegans* embryos over the columns. To detect KAL-1-binding HSPGs we digested eluates from the KAL-1 affinity column with heparitinase and probed blots with an antibody that recognizes HS 'stubs' generated by heparitinase digestion (Fig. 3C, WT lane). We consistently detected HSPGs of apparent molecular weight 50–56 kDa and ~35 kDa. Based on their elimination in extracts from mutants, these bands correspond to two isoforms of SDN-1 and a possible cleavage product of GPN-1 (Fig. 3 legend). Both SDN-1 and GPN-1 were eluted from KAL-1∷Fc columns by heparin, indicating that the binding is HS-dependent. Neither SDN-1 nor GPN-1 were enriched by control columns of Fc bound to protein A. Equal volumes of wild type extracts were analyzed as a loading control and were not enriched for SDN-1 or GPN-1 (Fig. 3C). As our genetic analysis suggested that C5 epimerization and 6-O-sulfation affected the KAL-1 pathway, we tested whether these modifications were required for the KAL-1/HSPG interaction. We found that HSPGs from *hse-5* or *hst-6* mutant extracts were not enriched by KAL-1∷Fc columns (Fig. 3C). We conclude that KAL-1 binds SDN-1 and GPN-1 via their HS side chains and that this binding requires the C5 epimerization and 6-O-sulfation of HS.

Syndecan SDN-1 and Glypican GPN-1 are expressed in ventral neuroblasts and have redundant roles in VNB migration

Our biochemical analyses indicated that KAL-1 interacts with at least two HSPGs, syndecan and glypican. We asked whether SDN-1 or GPN-1 were expressed during VNB migrations using transcriptional reporters (*gpn-1*, Fig. 4G; *sdn-1*-GFP not shown) and functional GFP-tagged constructs (see Materials and methods). SDN-1∷GFP transgenes were expressed in many ventral neuroblasts during their migrations, prior to and during epidermal enclosure (Figs. 4A–C); in later embryogenesis (Figs. 4D–F) SDN-1∷GFP was mainly expressed in the nervous system (nerve ring localization, nr) and pharynx (ph). GPN-1∷GFP was expressed in a smaller number of neuroblasts prior to epidermal enclosure (Figs. 4H, I). In later embryogenesis GPN-1∷GFP was expressed strongly in the developing pharynx (Figs. 4J–L) and in ventral cord neurons (Fig. 4L, arrows). As both cell surface HSPGs are expressed in ventral neuroblasts, KAL-1 could potentially interact with both, either on the same cells or on adjacent cells during VNB migrations.

We then tested whether HSPGs function in VNB migrations and whether they act in the KAL-1 pathway. *gpn-1(ok377)* mutants had delayed VNB migrations with a mean gastrulation cleft duration of 64 ± 3 min (Fig. 5). *kal-1 gpn-1* double mutants did not synergize (3.4% embryonic lethality; Table 2) whereas *efn-4 gpn-1* double mutants were synergistically enhanced (25.5% embryonic lethality) suggesting GPN-1, like KAL-1, acts in parallel to EFN-4 in embryogenesis. *kal-1 efn-4 gpn-1* triple mutants resembled *kal-1 efn-4* double mutants (41.9% and 35.9% embryonic lethality respectively). Thus, *kal-1* and *gpn-1* both enhance *efn-4*, but the triple mutant is not further enhanced relative to the most penetrant double mutant, consistent with *kal-1* and *gpn-1* affecting a common pathway. VNB migrations of *kal-1 gpn-1* double mutants were delayed compared to *kal-1* or *gpn-1* single mutants, suggesting GPN-1 also has KAL-1-independent functions in VNB migration (Fig. 5).

sdn-1 mutants display low penetrance morphogenetic defects (Table 2; Fig. 5). We compared the phenotypes caused by the *sdn-1* null mutation *zh20* (Rhiner et al., 2004) and the in-frame deletion allele *ok449*. *ok449* removes two of three predicted HS attachment sites (Minniti et al., 2004), and may eliminate HS-modified SDN-1. *sdn-1(zh20)* mutants displayed variably delayed VNB migrations, although this was not statistically significant; *sdn-1(ok449)* embryos had normal VNB migrations. Thus, SDN-1 is not individually required for VNB migrations. Both alleles of *sdn-1* strongly synergized with *efn-4* (Table 2); this synergism is stronger than that seen for *efn-4 kal-1* and implies that SDN-1 does not only interact with KAL-1. Indeed, *kal-1 efn-4 sdn-1* triple mutants were completely inviable. Both *zh20* and *ok449* caused slight enhancement of embryonic lethality in *kal-1* genetic backgrounds (7.9% and 8.3% respectively). However, VNB migrations of *kal-1 sdn-1(ok449)* were not significantly different from those of *kal-1* suggesting that the HS-dependent functions of SDN-1 in VNB migration affect the KAL-1 pathway. *kal-1 sdn-1(zh20)* double mutants displayed delayed VNB migrations relative to *kal-1*. Thus, SDN-1 appears to have at least two roles in VNB migration: an HS-dependent role, specifically affected in *ok449*, that may affect

Fig. 1. KAL-1 functions in ventral neuroblast movements. (A) Timelapse analyses of wild type (N2) and *kal-1(gb503)* embryos. In *C. elegans* gastrulation commences at ~100 min post first cell division, when the Ea and Ep cells ingress to the center of the embryo (arrowheads, 100 min time point). At about 200 min post first cell division, a transient depression, the gastrulation cleft, opens on the ventral surface of the embryo. The cleft is visible for ~55 min (dashed lines) in wt embryos, as mesodermal precursors enter the interior. In *kal-1* mutants, the cleft is visible for ~80 min (see 260 min). In this and all subsequent figures, anterior is to the left; views are ventral before enclosure and thereafter lateral; scale, 10 μm. (B) Expression of *kal-1* promoter transgene (*otIs33*) in VNBs during their migration towards the ventral midline (dashed line, 360 min). DIC (right panels) and GFP fluorescence (left) channels from timelapse movie. (C) Developmental timing in wild type and *kal-1* mutants. Early gastrulation events (Ea/p ingression to cleft opening) are normal in *kal-1* mutants (black bars). Closure of the cleft is delayed in *kal-1* mutants, which nevertheless undergo epidermal enclosure and reach comma stage slightly earlier than the wild type (white bars, $P < 0.05$ for N2 v *ok1056*; *t* test). (D) Gastrulation cleft duration in wild type, *kal-1* loss and gain of function, and *egl-15* null mutants. Cleft duration is significantly longer in *gb503* and *ok1056* loss of function mutants and in *otIs81* gain of function embryos compared to the wild type ($P < 0.0001$). *egl-15(n1456)* mutant embryos were derived from heterozygous *n1456/oxIs12* parents or from *n1456* homozygotes balanced by the *egl-15(+)* array *otEx1254*. Germline clones were identified as animals whose broods completely lacked expression of the GFP marker. VNB migration was not significantly different from the wild type in either situation. Number of embryos analyzed is shown within each bar. (E) VNB migration in null or strong loss of function mutations of the following genes: Eph receptor, *vab-1(e2027)*; canonical ephrin, *efn-1(e96)*; non-canonical ephrin, *efn-4 (bx80)*; LAR-related receptor tyrosine phosphatase, *ptp-3(op147)*; Robo, *mab-20(ev574)*. In all cases, double mutants with *kal-1(gb503)* (red bars) displayed significant delays in VNB migration compared to the single mutant ($P < 0.01$ for each pairwise comparison).

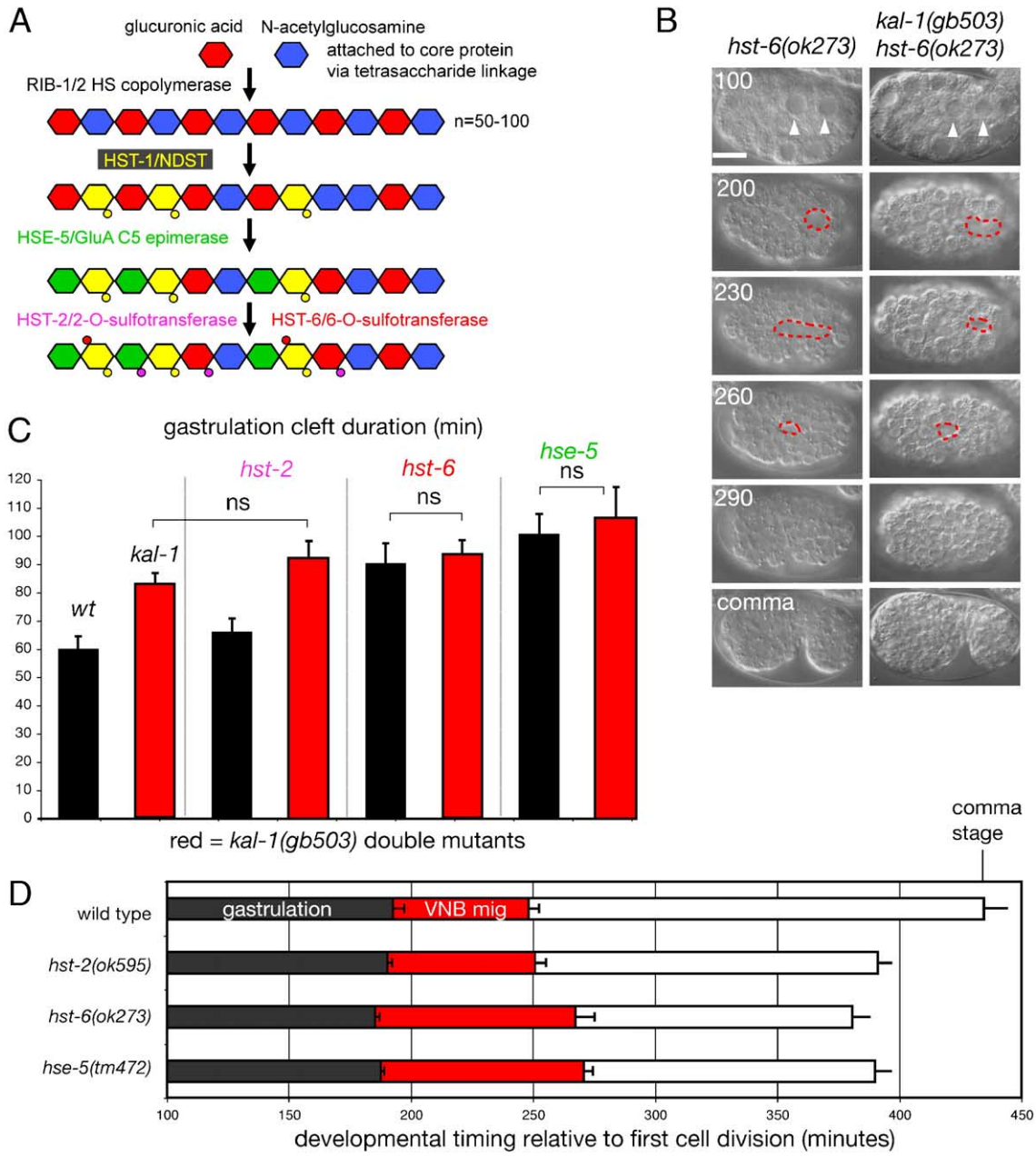

Fig. 2. Heparan sulfate modifications are required in VNB migrations. (A) Outline of HS synthesis in *C. elegans*. The first specific step in synthesis of HS GAG side chains is the addition of GlcNAc (blue) to the tetrasaccharide core. This commits the side chain to HS (rather than CS) synthesis and allows polymerization of the HS by Exostosin family copolymerases, represented in *C. elegans* by RIB-1 and RIB-2 (Morio et al., 2003). HST-1 is orthologous to GlcNAc N-deacetylase-N-sulfotransferase (NDST), which acts on regions of the nascent HS chain by de-acetylating N-acetyl glucosamine residues and replacing the acetyl group with a sulfate (yellow). HSE-5 is the *C. elegans* ortholog of glucuronyl C-5 epimerase, which epimerizes some GluA residues within the N-sulfated glucosamine regions to IdoA (green), providing flexibility to the HS chain. Finally, sulfotransferases HST-2/UroA-2-O-sulfotransferase, HST-3/GlcNS-3-O-sulfotransferase and HST-6/GlcNS-6-O-sulfotransferase provide additional sulfation of IdoA/GlcA and GlcNS residues. (B) Frames from 4D movies of *hst-6(ok273)* and *kal-1 hst-6* double mutants showing gastrulation cleft (red outline). (C) Gastrulation cleft duration in HS modification mutants and *kal-1* double mutants (red bars). Only *hst-6* and *hse-5* mutations cause longer cleft duration compared to wild type ($P < 0.005$ for each). These defects are not enhanced in double mutants with *kal-1*. (D) All HS modification mutants develop more rapidly from onset of gastrulation to comma stage. The reason for this accelerated development is not yet known, but suggests that HSPGs also affect later aspects of epidermal morphogenesis.

the KAL-1 pathway, and HS-independent roles (affected in the null mutant) that are independent of KAL-1.

Our analysis shows that SDN-1 and GPN-1 have cryptic functions in embryonic morphogenesis and VNB migrations. To ask whether SDN-1 and GPN-1 themselves act redundantly we examined *sdn-1 gpn-1* double mutants and found that they displayed delayed VNB migrations (Fig. 5) comparable to those of *kal-1* mutants (cleft duration of 81 ± 8 min). We conclude that SDN-1 and GPN-1 have partly redundant roles in VNB migration. To test the in vivo relationships between KAL-1 and the HSPG core proteins, we examined *kal-1 sdn-1 gpn-1* triple mutants. These triple mutants were not further enhanced

Table 2
Genetic interactions of *kal-1* with heparan sulfate modification enzyme and HSPG core protein mutations

Genotype	Embryonic lethality (%) ±SEM	Larval lethality (%) ±SEM	Adult Vab morphology (%) ±SEM
(A) HS modification enzymes			
Wild type	0.1 ± 0.1	0.1 ± 0.1	0.1 ± 0.2
kal-1(gb503)	0.6 ± 0.6 ns	0.2 ± 0.2 ns	5.6 ± 0.7***
efn-4(bx80)	11.5 ± 1.1	9.0 ± 1.8	31.2 ± 1.7
kal-1 efn-4	35.3 ± 4.2***	24.1 ± 2.5***	26.2 ± 1.4*
hst-2(ok595)	2.9 ± 1.6	0.4 ± 0.2	0.8 ± 0.2
kal-1 hst-2	1.5 ± 0.9 ns	3.2 ± 2.9 ns	2.0 ± 0.4 ns
efn-4 hst-2	52.9 ± 3.2	22.8 ± 1.5	20.1 ± 1.5
kal-1 efn-4 hst-2	81.0 ± 6.1***	12.6 ± 1.7***	2.5 ± 1.0***
hse-5(tm472)	5.9 ± 2.3	1.0 ± 0.4	12.6 ± 0.7
kal-1 hse-5	5.9 ± 1.7 ns	0.9 ± 0.3 ns	11.7 ± 1.2 ns
efn-4 hse-5	87.5 ± 5.9	10.1 ± 4.6	1.2 ± 0.9
kal-1 efn-4 hse-5	89.0 ± 3.8 ns	6.4 ± 0.7 ns	1.0 ± 0.3 ns
hst-6(ok273)	1.3 ± 0.6	0.0 ± 0.0	0.6 ± 0.3
kal-1 hst-6	1.7 ± 0.3 ns	0.0 ± 0.0 ns	2.6 ± 0.8 ns
efn-4 hst-6	58.5 ± 6.5	22.0 ± 1.7	13.0 ± 2.8
kal-1 efn-4 hst-6	66.2 ± 4.4 ns	22.2 ± 3.3 ns	10.3 ± 2.0 ns
(B) HS core protein mutations			
gpn-1(ok377)	3.5 ± 1.3	0.0 ± 0.0	0.8 ± 0.6
kal-1 gpn-1	3.4 ± 1.4 ns	0.4 ± 0.3 ns	3.3 ± 1.1 ns
efn-4(bx80)	11.5 ± 1.1	9.0 ± 1.8	31.2 ± 1.7
efn-4 gpn-1[a]	25.5 ± 5.5*	6.8 ± 1.1 ns	34.4 ± 3.9 ns
kal-1 efn-4 gpn-1	41.9 ± 6.8*	24.4 ± 2.1***	19.7 ± 4.0
sdn-1(ok449)	1.5 ± 0.7	0.3 ± 0.0	4.2 ± 1.0
kal-1 sdn-1 (ok449)	8.3 ± 1.7***	6.5 ± 2.0*	8.8 ± 1.0*
efn-4 sdn-1 (ok449)[a]	54.6 ± 6.2**	29.3 ± 3.2**	13.6 ± 2.0*
sdn-1(zh20)	2.5 ± 1.3	1.3 ± 0.7	4.8 ± 1.0
kal-1 sdn-1 (zh20)	7.9 ± 2.2 ns	3.0 ± 1.0 ns	10.3 ± 1.8*
efn-4 sdn-1 (zh20)[a]	62.8 ± 2.8***	27.9 ± 2.0***	6.8 ± 1.0***
gpn-1 sdn-1 (zh20)	2.8 ± 1.1	1.3 ± 0.2	5.0 ± 1.0
kal-1 gpn-1 sdn-1(zh20)	5.9 ± 1.2*	6.8 ± 1.3**	5.6 ± 1.1 ns

Embryonic lethality, larval lethality and adult epidermal morphology were scored in heparan sulfate modification and core protein mutants and in double and triple mutants with *kal-1(gb503)* or *efn-4(bx80)*. (A) *kal-1* and *efn-4* interactions with null mutations in HS modification enzyme genes. (B) *kal-1* and *efn-4* interactions with HSPG core protein mutations. $n > 500$ F1 animals (3–6 complete broods) for all genotypes. Significance values (*t* test, see Table 1) are between the matched *kal-1(+)* and *kal-1(−)* strains or between matched *efn-4(+)* and *efn-4(−)* strains ([a]).

beyond the strongest double mutant (Fig. 5; Table 2). Taken together, these genetic data are consistent with our biochemical results that KAL-1 interacts with both SDN-1 and GPN-1.

Discussion

Our goal was to identify the specific partners of KAL-1/Anosmin-1 in neuronal cell migrations. We find that the *C. elegans* anosmin-1 ortholog KAL-1 promotes the migrations of neuroblasts during embryogenesis. KAL-1 is broadly expressed in the ventral neuroblasts from mid gastrulation stages onwards. Although anosmin-1 has been implicated in FGF signaling, we find that FGF signaling does not act in VNB migrations, suggesting that KAL-1 does not modulate FGF signaling in *C. elegans*. Using double mutant analysis we show that KAL-1 action in neuroblast migration involves C5-epimerized and 6-O-sulfated HS chains attached to the cell surface HSPGs syndecan and glypican. These genetic results are consistent with our biochemical evidence for an HS-dependent interaction of KAL-1 with SDN-1 and GPN-1. This is the first demonstration of interactions of KAL-1/Anosmin-1 proteins with specific HSPGs and will allow the KAL-1/HSPG interaction to be manipulated by overexpression or misexpression of these core proteins.

The essential role of HSPGs in early development

Heparan sulfate proteoglycans have been implicated in numerous developmental processes and signaling pathways (Kramer and Yost, 2003; Lin, 2004). Insights into HSPG function have come from analysis of mutations affecting core proteins and of mutations in enzymes that catalyze synthesis and modification of HS side chains. The *C. elegans* complement of HSPGs is small relative to vertebrates, with known HSPG families represented by a single gene. *C. elegans* contains a single syndecan and at most two glypicans; a second *C. elegans* glypican-like protein, LON-2, does not appear to function in VNB migration (data not shown). The basement membrane HSPGs perlecan and type XVIII collagen have been characterized in detail, and do not appear to function in VNB migrations (not shown). The functions of *C. elegans* orthologs of two other HSPGs, the membrane protein agrin and the secreted protein testican, have not been reported.

In *C. elegans*, abrogation of HS synthesis confers dramatic defects in embryonic cell migrations. It is not yet understood why HS is essential for *C. elegans* embryogenesis, but this finding parallels results in other animals. In mice, deletion of the major HS glycosyltransferase Ext1 causes lethality at gastrulation and failure to form mesoderm, reflecting roles for HS in multiple signaling pathways (Lin et al., 2000). In *Drosophila*, lack of HS disrupts signaling in at least three pathways, Hedgehog, Wingless, and Dpp (Bornemann et al., 2004). In *C. elegans* only Wg signaling is known to be essential for embryogenesis, as it is required for induction of the gut. However gut induction and early embryogenesis appear normal in *rib* and *hst-1* mutants, suggesting that HS has essential functions in other pathways.

The functions of HSPGs in neural development have been explored in a variety of species. Tissue-specific deletion of Ext1 in the mouse CNS causes dramatic defects in neural development, attributed to reduced FGF and Slit signaling (Inatani et al., 2003). The tissue-autonomy of these defects further suggests that cell surface HSPGs are involved in CNS development. Reduced HS synthesis disrupts axon sorting in the zebrafish optic tract (Lee et al., 2004). The signaling

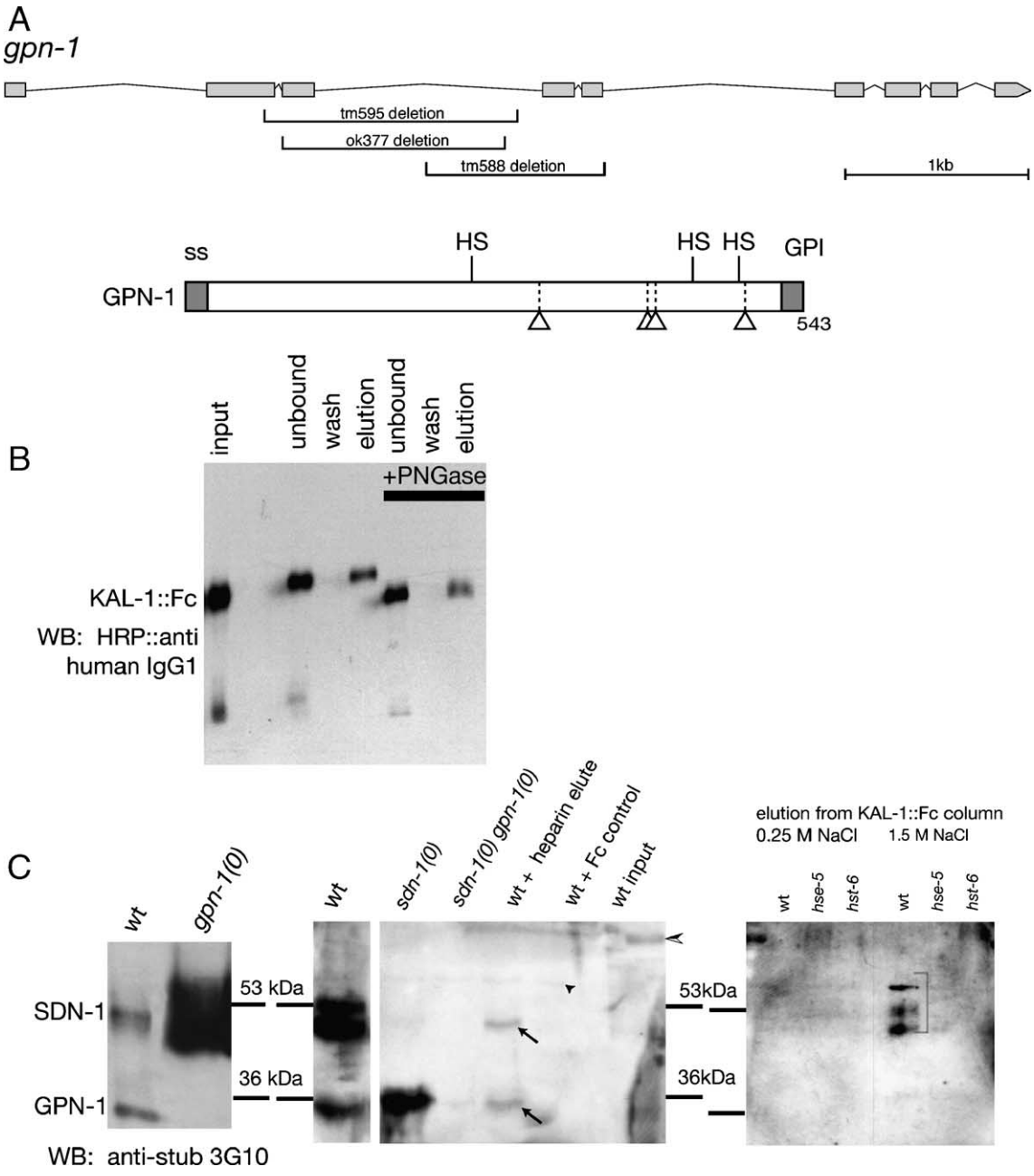

Fig. 3. KAL-1 binds GPN-1 and SDN-1 via an HS-dependent interaction. (A) The genomic structure of *gpn-1* and location of deletion alleles is shown. GPN-1 contains three predicted HS attachment sites (HS) and four potential cleavage sites for proprotein convertase (triangles) (B) KAL-1∷Fc expressed in 293T cells binds to heparin sepharose; removal of glycan moieties by N-glycosidase F (PNGase) reduced the molecular weight but did not abolish the HS interaction. (C) Extracts from *C. elegans* embryos were bound to KAL-1∷Fc columns, eluted with 1.5 M NaCl, and desalted on NAP5 sepharose columns. Eluted fractions were digested with heparatinase I to remove HS side chains, separated by SDS-PAGE, blotted and probed using the anti-HS stub monoclonal 3G10. Western blot of elutions of extracts from N2 (wild type) and *gpn-1(ok377)* mutant embryos. Approximately equal amounts of extract were applied. Two prominent bands are seen in the N2 lane at ~50 and ~30 kDa; the 50 kDa band corresponds to SDN-1 (Minniti et al., 2004); we identify the 30 kDa band as a GPN-1 product as it is absent from *gpn-1(ok377)* mutants. A weaker band at ~55 kDa appears to be an isoform of SDN-1. In extracts from wild type (N2; a longer exposure than in the right panel) and *sdn-1(zh20)* single mutants, and *sdn-1(zh20) gpn-1(ok377)* double mutant embryos, three major bands (solid arrows) are seen in the N2 lane, the 50 and 55 kDa bands are absent from the *sdn-1* lane, and all three bands are missing from the double mutant lane. A weak ~80 kDa band seen at approximately equal intensity in all samples (arrowhead) may correspond to the 80 kDa HSPG observed by Minniti et al. (2004). SDN-1 and GPN-1 from wild type extracts bound to KAL-1 columns were specifically eluted with 100 μg/ml heparin, showing that the KAL-1-HSPG interaction is HS-dependent. SDN-1 and GPN-1 were absent from eluates from an Fc control column. In extracts corresponding to the N2 input we see no enrichment for SDN-1 or GPN-1; a higher molecular weight HSPG is seen (large arrowhead) that does not correspond to any species enriched over KAL-1 columns, suggesting that KAL-1 interacts with specific HSPGs. Extracts were prepared from the wild type and from *hse-5* and *hst-6* mutants, bound to KAl-1∷Fc and eluted at low and high salt. Only wild type extracts contained KAL-1-interacting HSPGs.

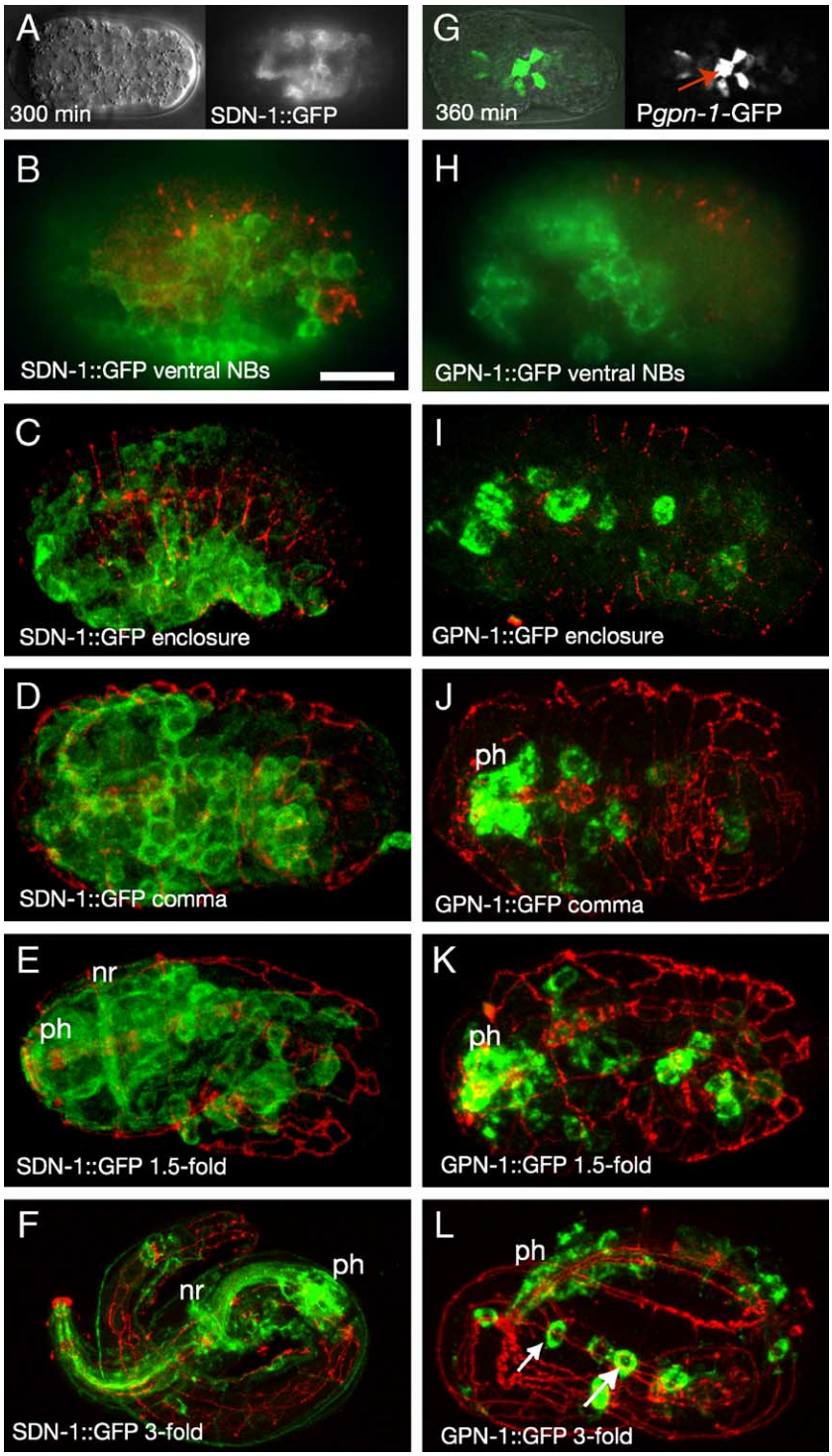

Fig. 4. SDN-1 and GPN-1 are expressed in the developing nervous system and pharynx. (A–F) Expression of functional SDN-1::GFP (*jtEx36*) in embryos during VNB migrations and epidermal enclosure. (A) DIC and GFP fluorescence of SDN-1::GFP in ventral neuroblasts prior to epidermal enclosure (300 min). (B–F) SDN-1::GFP (anti-GFP immunostaining, green) and epidermal adherens junctions (MH27, red) in embryos. (B), SDN-1::GFP is expressed in many ventral neuroblasts prior to epidermal sheet movement; ventral view. (C) SDN-1::GFP in ventral neurons at late enclosure. (D–F) SDN-1::GFP in neurons and pharynx (ph); SDN-1::GFP localization to the nerve ring (nr) is prominent. Panels C–F and I–L are projections of confocal Z-stacks. (G) P*gpn-1*::*GFP* (*juEx900*) is expressed in the developing pharynx and a small number of ventral neuroblasts (arrow) at bean stage (360 min). Expression is also occasionally seen in the gut and in 3–4 dorsal epidermal cells prior to enclosure. (H–L) Anti-GFP and MH27 immunostaining of functional GPN-1::GFP (*juEx1108*) in embryos. GPN-1::GFP is expressed in several ventral neuroblasts prior to epidermal sheet movement (H); in later stages GPN-1::GFP is confined to the pharynx (ph) and some ventral cord motor neurons (arrows, L). Scale, 10 μm.

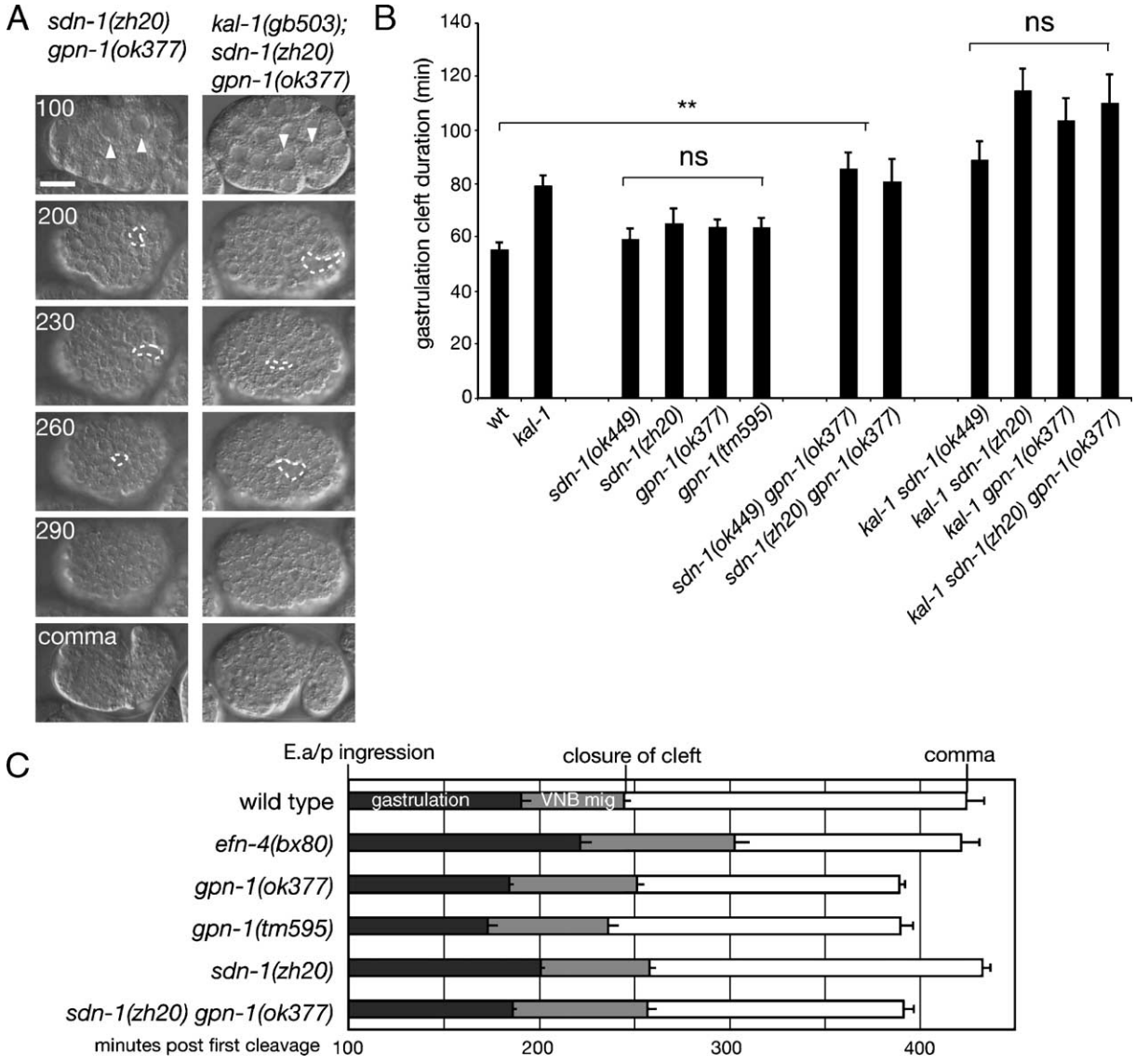

Fig. 5. SDN-1 and GPN-1 have redundant functions in neuroblast migrations. (A) 4-D panels from *sdn-1 gpn-1* double mutants and *kal-1 sdn-1 gpn-1* triple mutants showing lack of enhancement. (B) Quantitation of VNB migrations of *sdn-1* and *gpn-1* core protein mutants, either alone or in combination with *kal-1(gb503)*. *gpn-1* and *sdn-1* mutants show slightly delayed VNB migrations. *sdn-1(ok449) gpn-1(ok377)* and *sdn-1(zh20) gpn-1(ok377)* double mutants display delayed VNB migrations that resemble those of *kal-1* mutants. The *kal-1 sdn-1 gpn-1* triple mutant is not significantly enhanced relative to *kal-1 sdn-1(zh20)* or *kal-1 gpn-1* double mutants. (C) Developmental timing of HSPG core protein mutants during morphogenesis. *gpn-1(ok377)* shows accelerated development from gastrulation to comma stage similar to that of HS modification mutants. *sdn-1(zh20)* displays normal developmental timing, and does not enhance the *gpn-1* timing phenotype, suggesting that VNB migration and later morphogenesis are genetically separate events.

pathways dependent on HSPGs in axon sorting are not yet known; the roles of anosmin-1 in axon branching suggest that anosmin-1 is a candidate for these functions in optic tract development.

KAL-1, SDN-1 and GPN-1 promote movements of *C. elegans* ventral neuroblasts. KAL-1 is strongly expressed in the VNBs from early in development, and is likely to be present on the surfaces of VNBs as they move. Based on the overlapping expression of KAL-1, SDN-1, and GPN-1 in the VNBs, all three molecules may interact ‘in cis’ on the same cell surface (as shown in Fig. 6), or in trans, between adjacent neuroblasts. Both SDN-1 and GPN-1 (but not KAL-1) are strongly expressed in the developing pharynx. Pharyngeal precursors are internal to some ventral neuroblasts and could potentially provide a substrate for VNB migrations, with neuronally expressed KAL-1 interacting with pharyngeal HSPGs.

The roles of specific HS modifications

Mutations affecting HS modification enzymes should affect HS on multiple core proteins, and thus allow analysis of redundant functions of multiple HSPG core proteins. The effects of HS modification mutations on VNB migration are similar to those of *sdn-1 gpn-1* double mutants, suggesting that SDN-1 and GPN-1 may be the major core proteins involved. In general, lack of HS modifications has remarkably specific effects on *C. elegans* development (Bulow and Hobert, 2004;

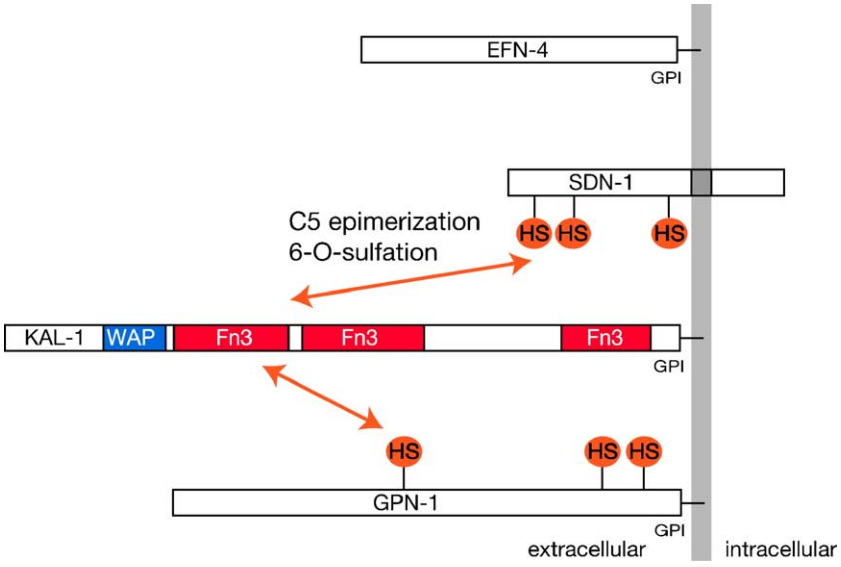

Fig. 6. Molecules and interactions involved in VNB migrations. Summary of interactions between KAL-1, SDN-1 and GPN-1 via HS side chains. Interactions are shown as occurring on the same membrane (in *cis*) but may also occur in *trans*, either between adjacent neuroblasts or between neuroblasts and pharyngeal precursors during VNB movements.

Kinnunen et al., 2005). This suggests that HS modifications have restricted roles, acting as specific surface codes for signaling molecules (Habuchi et al., 2004; Holt and Dickson, 2005). Our analysis of embryonic VNB migrations suggests that in this process KAL-1 interacts with HSPGs that are modified by HSE-5 and HST-6, but not by HST-2. This result is borne out by biochemical evidence that the KAL-1/HSPG interaction requires glucuronyl C5 epimerization and 6-O-sulfation. The KAL-1 gain of function axon branching phenotype in the AIY neurons likewise requires HSE-5 and HST-6, and is partly dependent on HST-2 (Bulow and Hobert, 2004). Thus, VNB migration and axon branching may involve KAL-1 interaction with similarly modified HSPGs. An apparent difference between the KAL-1 loss and gain of function phenotypes is that a KAL-1 gain of function epidermal morphogenesis phenotype, caused by pan-neural expression of KAL-1, is suppressed by *hse-5* but not by *hst-6* (Bulow et al., 2002). If 6-O-sulfation is required for KAL-1/HSPG interactions in VNB migration and AIY branching, why does lack of HST-6 not suppress the effects of pan-neural KAL-1? We hypothesize that pan-neural expression of KAL-1 combines both overexpression and misexpression, in contrast to overexpression in cells that normally express KAL-1 such as AIY. Pan-neural KAL-1 may therefore interact with HSPGs that it does not normally come into contact with. If such HSPGs are not 6-O-sulfated, loss of HST-6 activity may be insufficient to suppress the effects of KAL-1 misexpression.

The role of HSPGs in KAL-1/Anosmin-1 signaling

Why does KAL-1 function require HSPGs? An attractive model, based on the identification of FGFR1 mutations in autosomal dominant KS, has been that anosmin-1 signals via FGF receptors. The requirement for HSPGs in Anosmin-1 function could be thus explained by the important role for HS as a cofactor in FGF-FGFR interactions (Pellegrini, 2001). Our results suggest that this is not sufficient to account for the roles of KAL-1 in *C. elegans* VNB migrations, as we have been unable to detect a role for the FGFR in these cell migrations. Reduction in FGFR signaling also does not suppress the KAL-1 gain of function branching phenotype (Bulow et al., 2002). These results suggest that KAL-1 interacts with other receptors to regulate cell movement and branching.

Our results are more consistent with models whereby cell surface HSPGs anchor or localize KAL-1 so that it can act on extracellular matrix. Like anosmin-1, KAL-1 may locally activate ECM serine proteases (Hu et al., 2004), causing local degradation of ECM to promote ventral neuroblast migration and axonal branching. The apparent cell autonomy or local role of KAL-1 in branching and VNB migration imply that any effect on ECM must be highly localized to the surface of KAL-1-expressing cells. The migrations of ventral neuroblasts occur concurrently with early stages of basement membrane formation in *C. elegans* embryos (Huang et al., 2003), although it is not known if a basement membrane is necessary for VNB movements. The role of the ECM in modulating axonal branching also has yet to be tested. As the *C. elegans* genome does not encode the urokinase type plasminogen activator-like serine proteases linked to Anosmin-1 function, genetic and biochemical approaches will be required to find the ECM partners of KAL-1.

Acknowledgments

Some strains used in this work were obtained from the *Caenorhabditis* Genetic Center, which is supported by the NIH NCRR. We thank Yuji Kohara for cDNA clones, Andy Fire for vectors, and Takeshi Ishihara for the Venus clone. We are indebted to the *C. elegans* Gene Knockout Consortium and to Shohei Mitani and the Japanese National Bioresource Project

for generation of essential genetic mutations. We thank Hannes Bulow and Oliver Hobert for stimulating this project and for numerous reagents and advice, and Alex Hajnal for sharing *sdn-1(zh20)* before publication. We thank Yishi Jin for use of her confocal microscope and for comments on the manuscript. We thank members of the Jin and Chisholm laboratories for advice and support. T.K. was funded by the Wellcome Trust. Work in A.D.C.'s laboratory is supported by the US Public Health Service (NIH R01 GM54657).

Appendix A. Supplementary data

Supplementary data associated with this article can be found, in the online version, at doi:10.1016/j.ydbio.2006.02.036.

References

Ackley, B.D., Crew, J.R., Elamaa, H., Pihlajaniemi, T., Kuo, C.J., Kramer, J.M., 2001. The NC1/endostatin domain of *Caenorhabditis elegans* type XVIII collagen affects cell migration and axon guidance. J. Cell Biol. 152, 1219–1232.

Altun-Gultekin, Z., Andachi, Y., Tsalik, E.L., Pilgrim, D., Kohara, Y., Hobert, O., 2001. A regulatory cascade of three homeobox genes, *ceh-10*, *ttx-3* and *ceh-23*, controls cell fate specification of a defined interneuron class in *C. elegans*. Development 128, 1951–1969.

Andrenacci, D., Le Bras, S., Rosaria Grimaldi, M., Rugarli, E., Graziani, F., 2004. Embryonic expression pattern of the *Drosophila* Kallmann syndrome gene kal-1. Gene Expression Patterns 5, 67–73.

Bornemann, D.J., Duncan, J.E., Staatz, W., Selleck, S., Warrior, R., 2004. Abrogation of heparan sulfate synthesis in *Drosophila* disrupts the Wingless, Hedgehog and Decapentaplegic signaling pathways. Development 131, 1927–1938.

Brenner, S., 1974. The genetics of *Caenorhabditis elegans*. Genetics 77, 71–94.

Bulow, H.E., Hobert, O., 2004. Differential sulfations and epimerization define heparan sulfate specificity in nervous system development. Neuron 41, 723–736.

Bulow, H.E., Berry, K.L., Topper, L.H., Peles, E., Hobert, O., 2002. Heparan sulfate proteoglycan-dependent induction of axon branching and axon misrouting by the Kallmann syndrome gene *kal-1*. Proc. Natl. Acad. Sci. U. S. A. 99, 6346–6351.

Bulow, H.E., Boulin, T., Hobert, O., 2004. Differential functions of the *C. elegans* FGF receptor in axon outgrowth and maintenance of axon position. Neuron 42, 367–374.

Chin-Sang, I.D., George, S.E., Ding, M., Moseley, S.L., Lynch, A.S., Chisholm, A.D., 1999. The ephrin VAB-2/EFN-1 functions in neuronal signaling to regulate epidermal morphogenesis in *C. elegans*. Cell 99, 781–790.

Chin-Sang, I.D., Moseley, S.L., Ding, M., Harrington, R.J., George, S.E., Chisholm, A.D., 2002. The divergent *C. elegans* ephrin EFN-4 functions in embryonic morphogenesis in a pathway independent of the VAB-1 Eph receptor. Development 129, 5499–5510.

Chisholm, A.D., Hardin, J., 2005. Epidermal morphogenesis. In Wormbook, The *C. elegans* Research Community (Eds.). http://www.wormbook.org, Wormbook.

De Cat, B., Muyldermans, S.Y., Coomans, C., Degeest, G., Vanderschueren, B., Creemers, J., Biemar, F., Peers, B., David, G., 2003. Processing by proprotein convertases is required for glypican-3 modulation of cell survival, Wnt signaling, and gastrulation movements. J. Cell Biol. 163, 625–635.

Dode, C., Hardelin, J.P., 2004. Kallmann syndrome: fibroblast growth factor signaling insufficiency? J. Mol. Med. 82, 725–734.

Dode, C., Levilliers, J., Dupont, J.M., De Paepe, A., Le Du, N., Soussi-Yanicostas, N., Coimbra, R.S., Delmaghani, S., Compain-Nouaille, S., Baverel, F., Pecheux, C., Le Tessier, D., Cruaud, C., Delpech, M., Speleman, F., Vermeulen, S., Amalfitano, A., Bachelot, Y., Bouchard, P., Cabrol, S., Carel, J.C., Delemarre-van de Waal, H., Goulet-Salmon, B., Kottler, M.L., Richard, O., Sanchez-Franco, F., Saura, R., Young, J., Petit, C., Hardelin, J. P., 2003. Loss-of-function mutations in FGFR1 cause autosomal dominant Kallmann syndrome. Nat. Genet. 33, 463–465.

Finney, M., Ruvkun, G., 1990. The *unc-86* gene Product couples cell lineage and cell identity in *C. elegans*. Cell 63, 895–905.

Franco, B., Guioli, S., Pragliola, A., Incerti, B., Bardoni, B., Tonlorenzi, R., Carrozzo, R., Maestrini, E., Pieretti, M., Taillon-Miller, P., et al., 1991. A gene deleted in Kallmann's syndrome shares homology with neural cell adhesion and axonal path-finding molecules. Nature 353, 529–536.

George, S.E., Simokat, K., Hardin, J., Chisholm, A.D., 1998. The VAB-1 Eph receptor tyrosine kinase functions in neural and epithelial morphogenesis in *C. elegans*. Cell 92, 633–643.

Ghenea, S., Boudreau, J.R., Lague, N.P., Chin-Sang, I.D., 2005. The VAB-1 Eph receptor tyrosine kinase and SAX-3/Robo neuronal receptors function together during *C. elegans* embryonic morphogenesis. Development 132, 3679–3690.

Gonzalez-Martinez, D., Hu, Y., Bouloux, P.M., 2004a. Ontogeny of GnRH and olfactory neuronal systems in man: novel insights from the investigation of inherited forms of Kallmann's syndrome. Front. Neuroendocrinol. 25, 108–130.

Gonzalez-Martinez, D., Kim, S.H., Hu, Y., Guimond, S., Schofield, J., Winyard, P., Vannelli, G.B., Turnbull, J., Bouloux, P.M., 2004b. Anosmin-1 modulates fibroblast growth factor receptor 1 signaling in human gonadotropin-releasing hormone olfactory neuroblasts through a heparan sulfate-dependent mechanism. J. Neurosci. 24, 10384–10392.

Goodman, S.J., Branda, C.S., Robinson, M.K., Burdine, R.D., Stern, M.J., 2003. Alternative splicing affecting a novel domain in the *C. elegans* EGL-15 FGF receptor confers functional specificity. Development 130, 3757–3766.

Habuchi, H., Habuchi, O., Kimata, K., 2004. Sulfation pattern in glycosaminoglycan: does it have a code? Glycoconj. J. 21, 47–52.

Hardelin, J.P., Levilliers, J., del Castillo, I., Cohen-Salmon, M., Legouis, R., Blanchard, S., Compain, S., Bouloux, P., Kirk, J., Moraine, C., et al., 1992. X chromosome-linked Kallmann syndrome: stop mutations validate the candidate gene. Proc. Natl. Acad. Sci. U. S. A. 89, 8190–8194.

Hardelin, J.P., Levilliers, J., Blanchard, S., Carel, J.C., Leutenegger, M., Pinard-Bertelletto, J.P., Bouloux, P., Petit, C., 1993. Heterogeneity in the mutations responsible for X chromosome-linked Kallmann syndrome. Hum. Mol. Genet. 2, 373–377.

Hardelin, J.P., Julliard, A.K., Moniot, B., Soussi-Yanicostas, N., Verney, C., Schwanzel-Fukuda, M., Ayer-Le Lievre, C., Petit, C., 1999. Anosmin-1 is a regionally restricted component of basement membranes and interstitial matrices during organogenesis: implications for the developmental anomalies of X chromosome-linked Kallmann syndrome. Dev. Dyn. 215, 26–44.

Harrington, R.J., Gutch, M.J., Hengartner, M.O., Tonks, N.K., Chisholm, A.D., 2002. The C. elegans LAR-like receptor tyrosine phosphatase PTP-3 and the VAB-1 Eph receptor tyrosine kinase have partly redundant functions in morphogenesis. Development 129, 2141–2153.

Hebert, J.M., Lin, M., Partanen, J., Rossant, J., McConnell, S.K., 2003. FGF signaling through FGFR1 is required for olfactory bulb morphogenesis. Development 130, 1101–1111.

Holt, C.E., Dickson, B.J., 2005. Sugar codes for axons? Neuron 46, 169–172.

Hu, Y., Gonzalez-Martinez, D., Kim, S.H., Bouloux, P.M., 2004. Cross-talk of anosmin-1, the protein implicated in X-linked Kallmann's syndrome, with heparan sulphate and urokinase-type plasminogen activator. Biochem. J. 384, 495–505.

Huang, P., Stern, M.J., 2004. FGF signaling functions in the hypodermis to regulate fluid balance in *C. elegans*. Development 131, 2595–2604.

Huang, L.S., Tzou, P., Sternberg, P.W., 1994. The *lin-15* locus encodes two negative regulators of *Caenorhabditis elegans* vulval development. Mol. Biol. Cell 5, 395–411.

Huang, C.C., Hall, D.H., Hedgecock, E.M., Kao, G., Karantza, V., Vogel, B.E., Hutter, H., Chisholm, A.D., Yurchenco, P.D., Wadsworth, W.G., 2003. Laminin alpha subunits and their role in *C. elegans* development. Development 130, 3343–3358.

Ikegami, R., Zheng, H., Ong, S.H., Culotti, J., 2004. Integration of semaphorin-2A/MAB-20, ephrin-4, and UNC-129 TGF-beta signaling pathways regulates sorting of distinct sensory rays in *C. elegans*. Dev. Cell 6, 383–395.

Inatani, M., Irie, F., Plump, A.S., Tessier-Lavigne, M., Yamaguchi, Y., 2003. Mammalian brain morphogenesis and midline axon guidance require heparan sulfate. Science 302, 1044–1046.

Key, B., St John, J., 2002. Axon navigation in the mammalian primary olfactory pathway: where to next? Chem. Senses 27, 245–260.

Kinnunen, T., Huang, Z., Townsend, J., Gatdula, M.M., Brown, J.R., Esko, J.D., Turnbull, J.E., 2005. Heparan 2-O-sulfotransferase, *hst-2*, is essential for normal cell migration in *Caenorhabditis elegans*. Proc. Natl. Acad. Sci. U. S. A. 102, 1507–1512.

Kramer, K.L., Yost, H.J., 2003. Heparan sulfate core proteins in cell–cell signaling. Annu. Rev. Genet. 37, 461–484.

Lee, J.S., von der Hardt, S., Rusch, M.A., Stringer, S.E., Stickney, H.L., Talbot, W.S., Geisler, R., Nusslein-Volhard, C., Selleck, S.B., Chien, C.B., Roehl, H., 2004. Axon sorting in the optic tract requires HSPG synthesis by ext2 (dackel) and extl3 (boxer). Neuron 44, 947–960.

Legouis, R., Hardelin, J.P., Levilliers, J., Claverie, J.M., Compain, S., Wunderle, V., Millasseau, P., Le Paslier, D., Cohen, D., Caterina, D., et al., 1991. The candidate gene for the X-linked Kallmann syndrome encodes a protein related to adhesion molecules. Cell 67, 423–435.

Lin, X., 2004. Functions of heparan sulfate proteoglycans in cell signaling during development. Development 131, 6009–6021.

Lin, X., Wei, G., Shi, Z., Dryer, L., Esko, J.D., Wells, D.E., Matzuk, M.M., 2000. Disruption of gastrulation and heparan sulfate biosynthesis in EXT1-deficient mice. Dev. Biol. 224, 299–311.

MacColl, G., Bouloux, P., Quinton, R., 2002. Kallmann syndrome: adhesion, afferents, and anosmia. Neuron 34, 675–678.

Minniti, A.N., Labarca, M., Hurtado, C., Brandan, E., 2004. *Caenorhabditis elegans* syndecan (SDN-1) is required for normal egg laying and associates with the nervous system and the vulva. J. Cell Sci. 117, 5179–5190.

Morio, H., Honda, Y., Toyoda, H., Nakajima, M., Kurosawa, H., Shirasawa, T., 2003. EXT gene family member *rib-2* is essential for embryonic development and heparan sulfate biosynthesis in *Caenorhabditis elegans*. Biochem. Biophys. Res. Commun. 301, 317–323.

Nagai, T., Ibata, K., Park, E.S., Kubota, M., Mikoshiba, K., Miyawaki, A., 2002. A variant of yellow fluorescent protein with fast and efficient maturation for cell-biological applications. Nat. Biotechnol. 20, 87–90.

Nance, J., Priess, J.R., 2004. Gastrulation in nematodes. In: Stern, C.D. (Ed.), Gastrulation: from Cells to Embryo. Cold Spring Harbor Laboratory Press, Cold Spring Harbor, NY, pp. 51–61.

Pellegrini, L., 2001. Role of heparan sulfate in fibroblast growth factor signalling: a structural view. Curr. Opin. Struct. Biol. 11, 629–634.

Rhiner, C., Gysi, S., Frohli, E., Hengartner, M.O., Hajnal, A., 2005. Syndecan regulates cell migration and axon guidance in *C. elegans*. Development 132, 4621–4633.

Rogalski, T.M., Williams, B.D., Mullen, G.P., Moerman, D.G., 1993. Products of the *unc-52* gene in *Caenorhabditis elegans* are homologous to the core protein of the mammalian basement membrane heparan sulfate proteoglycan. Genes Dev. 7, 1471–1484.

Rugarli, E.I., 1999. Kallmann syndrome and the link between olfactory and reproductive development. Am. J. Hum. Genet. 65, 943–948.

Rugarli, E.I., Di Schiavi, E., Hilliard, M.A., Arbucci, S., Ghezzi, C., Facciolli, A., Coppola, G., Ballabio, A., Bazzicalupo, P., 2002. The Kallmann syndrome gene homolog in *C. elegans* is involved in epidermal morphogenesis and neurite branching. Development 129, 1283–1294.

Schwanzel-Fukuda, M., Bick, D., Pfaff, D.W., 1989. Luteinizing hormone-releasing hormone (LHRH)-expressing cells do not migrate normally in an inherited hypogonadal (Kallmann) syndrome. Brain Res. Mol. Brain Res. 6, 311–326.

Soussi-Yanicostas, N., Hardelin, J.P., Arroyo-Jimenez, M.M., Ardouin, O., Legouis, R., Levilliers, J., Traincard, F., Betton, J.M., Cabanie, L., Petit, C., 1996. Initial characterization of anosmin-1, a putative extracellular matrix protein synthesized by definite neuronal cell populations in the central nervous system. J. Cell Sci. 109 (Pt. 7), 1749–1757.

Soussi-Yanicostas, N., Faivre-Sarrailh, C., Hardelin, J.P., Levilliers, J., Rougon, G., Petit, C., 1998. Anosmin-1 underlying the X chromosome-linked Kallmann syndrome is an adhesion molecule that can modulate neurite growth in a cell-type specific manner. J. Cell Sci. 111 (Pt. 19), 2953–2965.

Soussi-Yanicostas, N., de Castro, F., Julliard, A.K., Perfettini, I., Chedotal, A., Petit, C., 2002. Anosmin-1, defective in the X-linked form of Kallmann syndrome, promotes axonal branch formation from olfactory bulb output neurons. Cell 109, 217–228.

Withee, J., Galligan, B., Hawkins, N., Garriga, G., 2004. *Caenorhabditis elegans* WASP and Ena/VASP proteins Play compensatory roles in morphogenesis and neuronal cell migration. Genetics 167, 1165–1176.